

# Magnetorotational instability in weakly ionised, stratified accretion discs

Raquel Salmeron

*School of Physics, University of Sydney, NSW 2006, Australia*

Mark Wardle

*Physics Department, Macquarie University, NSW 2109, Australia*

2003 April 21

**Abstract.** We present a linear analysis of the vertical structure and growth of the magnetorotational instability in weakly ionised, stratified accretion discs. The method includes the effects of the magnetic coupling, the conductivity regime of the fluid and the strength of the magnetic field, which is initially vertical. The conductivity is treated as a tensor and assumed constant with height.

The Hall effect causes the perturbations to grow faster and act over a much more extended section of the disc when the magnetic coupling is low. As a result, significant accretion can occur closer to the midplane, despite the weak magnetic coupling, because of the high column density of the fluid. This is an interesting alternative to the commonly held view that accretion is relevant mainly in the surface regions of discs, which have a better coupling, but a much lower fluid density.

**Keywords:** accretion discs, instabilities, magnetohydrodynamics

## 1. Introduction

The magnetorotational instability (MRI) (Balbus & Hawley 1991(BH91 hereafter), Hawley & Balbus 1991) transports angular momentum radially outwards in accretion discs through the distortion of the magnetic field lines that connect fluid elements. In protostellar discs, low conductivity is important, specially in the inner regions (Gammie 1996; Wardle 1997). As a result, low  $k$  modes are relevant and vertical stratification is a key factor of the analysis. However, most models of the MRI in these environments have adopted either the ambipolar diffusion or resistive approximations and have not simultaneously treated stratification and Hall conductivity. We present here a linear analysis of the MRI, including the Hall effect, in a stratified disc.

## 2. Formulation

We write the equations of non-ideal MHD about a local keplerian frame corotating with the disc at the angular frequency  $\Omega$ . The velocity field



© 2018 Kluwer Academic Publishers. Printed in the Netherlands.

is expressed as a departure from exact keplerian motion,  $\mathbf{v} = \mathbf{V} - \mathbf{v}_K$ , where  $\mathbf{V}$  is the velocity in the standard laboratory frame  $(r, \phi, z)$  and  $\mathbf{v}_K$  is the keplerian velocity at the radius  $r$ . We assume the fluid is weakly ionised, meaning that the abundances of charged species are low enough that their inertia and thermal pressure can be neglected, together with the effects of ionisation and recombination processes in the neutral gas. Under these conditions, separate equations of motion for the charged species are not required and the fluid equations are:

$$\frac{\partial \rho}{\partial t} + \nabla \cdot (\rho \mathbf{v}) = 0, \quad (1)$$

$$\frac{\partial \mathbf{v}}{\partial t} + (\mathbf{v} \cdot \nabla) \mathbf{v} - 2\Omega v_\phi \hat{\mathbf{r}} + \frac{1}{2}\Omega v_r \hat{\phi} - \frac{v_K^2}{r} \hat{\mathbf{r}} + \frac{c_s^2}{\rho} \nabla \rho + \nabla \Phi = \frac{\mathbf{J} \times \mathbf{B}}{c\rho}, \quad (2)$$

$$\frac{\partial \mathbf{B}}{\partial t} = \nabla \times (\mathbf{v} \times \mathbf{B}) - c \nabla \times \mathbf{E}' - \frac{3}{2}\Omega \mathbf{B}_r \hat{\phi}. \quad (3)$$

In the equation of motion (2),  $\Phi$  is the gravitational potential for a non self-gravitating disc and  $\mathbf{v}_K^2/r$  is the centripetal term generated by keplerian motion. Coriolis terms  $2\Omega v_\phi \hat{\mathbf{r}}$  and  $\frac{1}{2}\Omega v_r \hat{\phi}$  are associated with the use of a local keplerian frame and  $c_s$  is the isothermal sound speed. In the induction equation (3),  $\mathbf{E}'$  is the electric field in the frame comoving with the neutrals and  $\frac{3}{2}\Omega \mathbf{B}_r \hat{\phi}$  accounts for the generation of toroidal by differential rotation. Additionally, the magnetic field must satisfy the constraint  $\nabla \cdot \mathbf{B} = 0$  and the current density must satisfy Ampere and Ohm's laws. Following Wardle & Ng (1999), Wardle 1999 (W99) and references therein, the current density is expressed as,

$$\mathbf{J} = \sigma \cdot \mathbf{E}' = \sigma_{\parallel} \mathbf{E}'_{\parallel} + \sigma_1 \hat{\mathbf{B}} \times \mathbf{E}'_{\perp} + \sigma_2 \mathbf{E}'_{\perp}, \quad (4)$$

where  $\mathbf{E}'_{\parallel}$  and  $\mathbf{E}'_{\perp}$  are the components of  $\mathbf{E}'$  parallel and perpendicular to  $\mathbf{B}$ . Note that the conductivity is a tensor with components  $\sigma_{\parallel}$ , parallel to the magnetic field,  $\sigma_1$ , the Hall conductivity, and  $\sigma_2$ , the Pedersen conductivity.

Our model includes vertical stratification, but it is local in the radial direction. The vertical density distribution in hydrostatic equilibrium is  $\rho/\rho_o = \exp(-z^2/2H^2)$  where  $\rho_o$  is the midplane gas density and  $H = c_s/\Omega$  is the scaleheight of the disc. Equations (1) to (4) were linearised about an initial steady state where  $\mathbf{J} = \mathbf{v} = \mathbf{E}' = 0$  and  $\mathbf{B} = B\hat{z}$ . Note that as  $\mathbf{E}'$  vanishes in the initial state, the changes in the conductivity due to the MRI are not relevant in this linear formulation and only the unperturbed values of  $\sigma$  are required. Taking perturbations of the form  $\mathbf{q} = \mathbf{q}_0 + \delta\mathbf{q}(z)e^{i\omega t}$  and assuming  $k = k_z$  we obtained a system

of ordinary differential equations (ODE) in  $\delta\mathbf{E}$  (the perturbations of the electric field in the laboratory frame),  $\delta\mathbf{B}$ , and the growth rate  $\nu = i\omega/\Omega$ . Three parameters control the evolution of the fluid. (1)  $v_A/c_s$ , the ratio of the Alfvén speed and the isothermal sound speed of the gas at the midplane, which is a measure of the strength of the magnetic field. (2)  $\chi_o$ , the ratio of the frequency above which flux-freezing breaks down and the dynamical frequency of the disc. When  $\chi_o < 1$  the magnetic field is poorly coupled to the disc. (3)  $\sigma_1/\sigma_2$ , the ratio of the conductivity terms perpendicular to the magnetic field, which characterises the *conductivity regime* of the fluid.

We present here results associated with the *ambipolar diffusion* limit ( $\sigma_1 = 0$ ), both *Hall* limits ( $\sigma_2 = 0$ ,  $\sigma_1 B_z > 0$  and  $\sigma_1 B_z < 0$ ) and the *full conductivity* regime ( $\sigma_1 = \sigma_2$ ). Ambipolar diffusion is dominant at relatively low densities, when the magnetic field is frozen into the ionised component of the fluid. Conversely, Hall limits are predominant at intermediate densities, and are characterised by a varying degree of magnetic coupling amongst charged species. Typically electrons are well coupled, but ions and especially grains tend to be tied to the neutrals via collisions. We note that the *Ohmic* regime, which dominates at low densities, when the charged species are attached to the neutrals via collisions, is identical to the ambipolar diffusion regime for the modes of interest here. We integrated this system of equations vertically as a two-point boundary value problem for coupled ODE with boundary conditions  $\delta B_r = \delta B_\phi = 0$  and  $\delta E'_r = 1$  at  $z = 0$  and  $\delta B_r = \delta B_\phi = 0$  at  $z/H = 5$ . We refer the reader to Salmeron & Wardle (in press), for full details of the method and results.

### 3. RESULTS

We compare the structure and growth rate of MRI perturbations as a function of the magnetic coupling  $\chi_o$  for different conductivity regimes and  $v_A/c_s = 0.1$  (Fig. 1). At very high magnetic coupling ( $\chi_o \approx 100$ ), ideal MHD holds and all conductivity regimes are alike (see leftmost column of the figure). For a weaker coupling, such that  $\chi_o > v_A/c_s$ , the structure of the ambipolar diffusion limit and full conductivity regimes is similar, signalling that ambipolar diffusion is dominant in this region of parameter space. Note that both perturbations peak at the node closest to the surface. This occurs because the maximum growth rate of ambipolar diffusion perturbations increases with the local  $\chi$  (W99), which in turn is a function of height. As a result, at higher  $z$  the local growth of the instability increases, driving the amplitude of these global perturbations to increase. Hall perturbations, on the other hand, peak

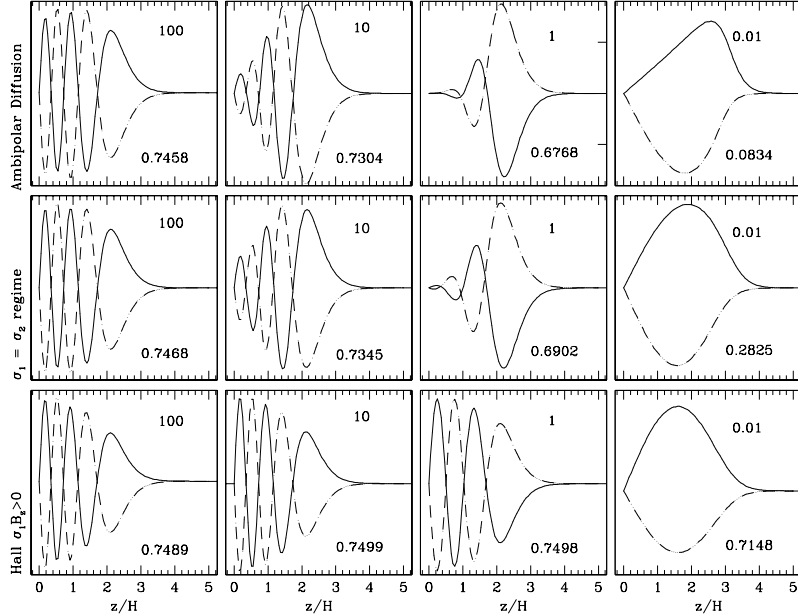


Figure 1. Structure and growth rate (shown in the lower right corner of each panel) of the most unstable modes of the MRI for different conductivity regimes as a function of  $\chi_o$  (indicated at the top right corner). In all cases  $v_A/c_s = 0.1$ .

at the node closest to the midplane, as  $\nu_{max}$  is the same for all  $\chi$  (W99) in this case and the instability is not driven from any particular vertical location. Finally, for  $\chi_o < v_A/c_s$  (rightmost column), ambipolar diffusion is damped (W99) and the MRI is driven by the Hall effect. In this case ambipolar diffusion and full conductivity perturbations differ, the structure of the latter ones resembling the Hall limit, as expected.

We also explored the growth rate of the perturbations in parameter space. Fig. 2 (left panel) shows the growth rate of the most unstable perturbations ( $\nu_{max}$ ) as a function of  $\chi_o$  for ambipolar diffusion and both Hall limits with  $v_A/c_s = 0.1$ . At good coupling the instability grows at  $\sim 0.75\Omega$  in all cases. As  $\chi_o$  diminishes,  $\nu_{max}$  is reduced at a rate that depends on the conductivity regime. The maximum growth rate departs significantly from the ideal value for  $\chi_o \sim 0.1$  (ambipolar diffusion regime) and for  $\chi_o \sim 0.01$  (Hall  $\sigma_1 B_z > 0$  limit). The Hall  $\sigma_1 B_z < 0$  case could not be analysed for  $\chi_o < 2$  because in this region of parameter space all wavenumbers grow (W99) and our code fails to converge. These results are consistent with the finding that ambipolar diffusion modes grow when  $\chi \gtrsim v_A/c_s$  while Hall cases require  $\chi \gtrsim v_A^2/c_s^2$  (W99). As a result, for  $\chi_o < v_A/c_s$  ambipolar diffusion perturbations have negligible growth, but when Hall conductivity is present the instability still grows at  $\nu = 0.2 - 0.3$  (see Fig. 1). In fact,

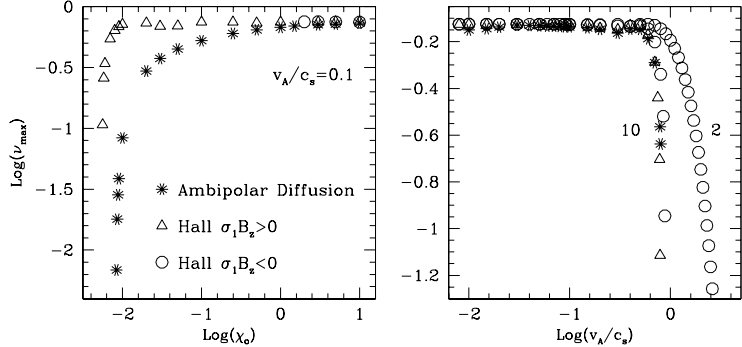


Figure 2. Maximum growth of the MRI. Left: as a function of  $\chi_o$  with  $v_A/c_s = 0.1$ . Right: as a function of  $v_A/c_s$  for  $\chi_o = 10$  and  $\chi_o = 2$  (Hall  $\sigma_1 B_z < 0$  regime only)

we found that when Hall terms dominate,  $\nu \sim 0.75$  for  $\chi_o \sim 10^{-4}$  even at  $v_A/c_s \sim 0.01$ , as expected.

Fig. 2 (right panel) shows the maximum growth rate as a function of  $v_A/c_s$  for  $\chi_o = 10$  and 2 (the latter one for Hall  $\sigma_1 B_z < 0$  regime only). For very weak  $v_A/c_s$ , the MRI grows at close to the ideal rate in all regimes. Generally, increasing the strength of the magnetic field has little effect on  $\nu_{\max}$  until  $v_A/c_s \sim 1$ , when all perturbations are damped (e.g. see Fig. 2,  $\chi_o = 10$ ). At this  $v_A/c_s$ , the wavelength of the most unstable modes becomes  $\sim H$ , the scaleheight of the disc (BH91). An exception to this occurs in the Hall  $\sigma_1 B_z < 0$  regime for  $\chi_o = 2$ . In this case we found unstable modes for  $v_A/c_s$  up to 2.9. We know from the local analysis (W99) that once the local  $\chi < 2$ , unstable modes exist for every  $k v_A / \Omega$  in this regime. As a result, even for suprathermal fields ( $v_A/c_s > 1$ ), there are still unstable modes with  $kH \lesssim 1$  growing within the disc.

#### 4. Discussion

In a real disc, different conductivity regimes are expected to dominate at different heights. Despite this, it is common to neglect the contribution of Hall terms in studies of non-ideal accretion discs, which generally adopt either the ambipolar diffusion or resistive approximations. To illustrate the way Hall conductivity can affect the dynamics and evolution of the fluid we modelled the MRI with a set of parameters such that the Hall regime dominates closer to the midplane while ambipolar diffusion is predominant near the surface, as expected to occur in a real disc. We compared these results with the ambipolar diffusion approximation (see Fig. 3). Note that in the full conductivity case the extent of the dead zone is reduced and the growth rate is increased in relation to the

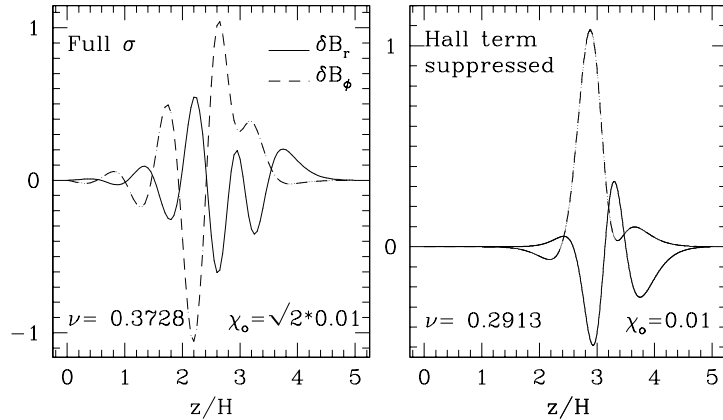


Figure 3. Structure and growth rate of the MRI when the Hall regime is dominant close to the midplane and ambipolar diffusion dominates near the surface (left panel) and under the ambipolar diffusion approximation (right panel).  $v_A/c_s = 0.01$ .

ambipolar diffusion limit. This has implications for the global evolution of the disc, specially considering that even though the MRI is damped in the dead zone, velocity fluctuations persist, driven by turbulence in the active zones, and transport angular momentum through non-axisymmetric density waves (Stone & Fleming 2003). On the other hand, a quiescent zone would allow dust grains to settle towards the midplane and begin to assemble into planetesimals (e.g Weidenschilling & Cuzzi 1993), so the process of planet formation could also be affected by Hall conductivity.

Clearly, more detailed modelling is required. The assumption of constant conductivity is unrealistic and will affect the nature of the global modes. An analysis including a  $z$ -dependent conductivity is underway to examine more fully the MRI in low conductivity discs and to quantify the importance of Hall terms.

## References

Balbus S. A., Hawley J. F., 1991, ApJ, 376, 214  
 Gammie C. F., 1996, ApJ, 457, 355  
 Hawley J. F., Balbus S. A., 1991, ApJ, 376, 223  
 Salmeron R., Wardle M., MNRAS, in press  
 Stone J., Fleming T., 2003, ApJ, in press  
 Wardle M., 1997, in Proc. IAU Colloq. 163, ed. D. Wickramasinghe, L. Ferrario, G. Bicknell (San Francisco: ASP), p. 561  
 Wardle M., 1999, MNRAS, 307, 849 (W99)  
 Wardle M., Ng C., 1999, MNRAS, 303, 239  
 Weidenschilling S. J., Cuzzi J. N., 1993, in Protostars & Planets III, ed. E. H. Levy, J. I. Lunine (Tucson: Univ. Arizona Press), p. 1031